

POSITION RESOLUTION OF OPTICAL FIBRE-BASED BEAM LOSS MONITORS USING LONG ELECTRON PULSES

E. Nebot del Busto, M. Kastriotou, CERN, Geneva, Switzerland & University of Liverpool, UK
 M.J. Boland, ASCo, Clayton & The University of Melbourne, Australia
 R.P. Rasool, The University of Melbourne, Australia
 W. Farabolini, CERN, Geneva, Switzerland & CEA/DSM/IRFU, Saclay, France
 S. Doerbert, E. Effinger, E. B. Holzer, F.S. Domingues, W. Viganò, CERN, Geneva, Switzerland
 C.P. Welsch Cockcroft Institute, Warrington; University of Liverpool, UK

Abstract

Beam loss monitoring systems based on optical fibres (oBLM), have been under consideration for future colliders for several years. To distinguish losses between consecutive quadrupoles, the position resolution of detected losses is required to be less than 1 m. A resolution of better than 0.5 m has been achieved in machines with single, short pulses of the order of a nanosecond. In the case of longer beam pulses with 150 ns duration, as they would be in the Compact Linear Collider (CLIC), the longitudinal length of signals in the fibre is close to the duration of the beam pulse which makes loss reconstruction very challenging. In this contribution results from experiments into the position resolution of an oBLM system based on long beam pulses are presented. These measurements have been performed at the CLIC Test Facility (CTF3) at CERN and the Australian Synchrotron Light Source (ASLS). In the former, controlled beam losses were created in a 22.5 m long decelerating Test Beam Line (TBL) LINAC. In the latter, loss localization was studied by comparing that from single bunches with those from longer bunch trains. In both cases the losses were detected using a 200 μm core pure silica fibre coupled to a Silicon Photomultiplier (SiPM) photon detector.

INTRODUCTION

The operation of particle accelerators would not be possible without the use of instruments and diagnostics systems that allow the main properties of the beam to be characterized. Beam Loss Monitors (BLM), particle detectors installed outside of the vacuum chamber to detect beam induced showers, are a powerful tool for the optimization of the performance of a machine as well as for protecting it against damage. Over the past ten years, optical fibre based BLM (oBLM) systems have been studied and implemented in several accelerator facilities [1] due to the various advantages that they bring with respect to standard BLM techniques. The prompt nature of the Cherenkov light generated in the fibre by the crossing of a high energy charged particle provides a very fast detection technique, with the main limitation coming from dispersive effects in the fibre core. Moreover, only photons with energies above the electron-positron generation threshold would (indirectly) generate light. This is particularly interesting in synchrotron light sources where the large number of low energy photons can

limit the sensitivity of BLM systems. From a machine protection perspective, an optical fibre may provide coverage of a full beam line preventing any potentially dangerous beam losses from going undetected. In this contribution, the determination of the original location of beam losses via the time of flight of photons in the fibre core of oBLM systems is discussed. Several experiments conducted at the Australian Synchrotron Light Source (ASLS) and the CLIC Test Facility at CERN (CTF3) with single electron bunches and long multi-bunch pulses are presented.

THE MACHINES

This section describes the most important features of the two facilities where the presented studies were conducted.

The Australian Synchrotron Light Source

The Australian Synchrotron [2] can be schematically seen on the right side of Figure 1. A thermionic gun injects electrons into a 14 m LINAC equipped with two 3 GHz normal conducting RF cavities that accelerate electrons up to 100 MeV. The particle energies are increased up to 3 GeV in a 130 m Booster ring equipped with 500 MHz RF cavities. Electrons are finally injected into a 216 m storage ring, also equipped with 500 MHz normal conducting cavities. The storage ring is subdivided into 14 sectors, each one of them containing a double bend achromat cell and a straight section. In Vacuum Undulators (IVU) are installed in the straight sections of sectors 3, 5 and 13, and the RF cavities in sectors 6 and 7. Sector 11 is equipped with beam scrapers to protect the insertion devices by concentrating beam losses at this location. The machine provides a flexibility to tune the beam conditions used for these experiments. The bunch charge can be varied from 10^{+5} – 10^{+9} [4], the bucket in which a single bunch will be injected can be chosen and injection of up to 75 bunches is possible.

The Test Beam Line at CTF3

CTF3 was designed and constructed to verify the feasibility of the novel two-beam acceleration concept of the Compact Linear Collider (CLIC) [3]. A thermionic gun and a bunching system provide an electron pulse with a peak current of 3.0 A and a length that can vary from 0.1 to 1.4 μm . Four normal conducting RF structures boost the electron energies up to 120 MeV. Particles are then driven towards a small delay loop and a storage ring that may be used for

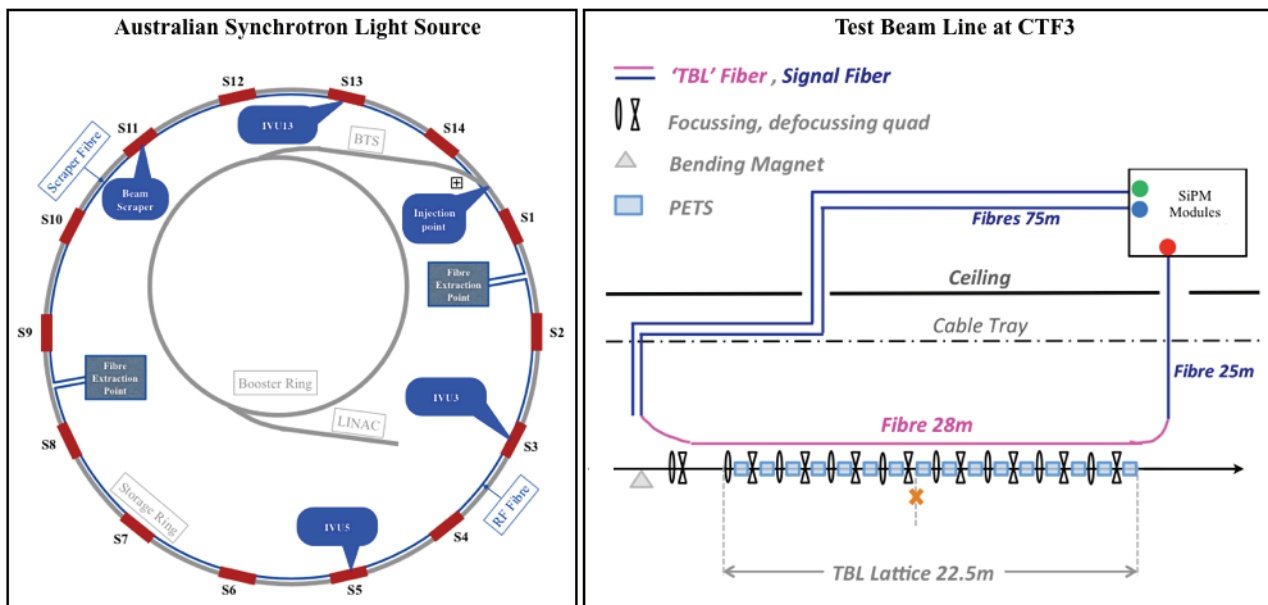


Figure 1: Simplified sketch of ASLS, the TBL and the respective optical fibre installations.

shortening the injected beam pulse and increasing the peak current. These pulses are then directed to the experimental hall where the TBL, shown on the left side of Figure 1, is located. The TBL [5] is a 22.5 meter long decelerating LINAC that is composed of eight 2.8 meter long FODO cells that feature two quadrupoles, two Beam Position Monitors (BPM) and two Power Extraction and Transfer Structures (PETS). The BPMs at the TBL [6] provide the only beam current measurement device along the line with an accuracy of around 10 %.

OPTICAL FIBRE BLM SYSTEM

The prototype oBLM system used for the experiments described in this document is composed of three main parts, namely: the active detector (fibre), the front-end electronics and the back-end electronics. The optical fibres have a pure silica 200 (245) μm core (cladding) and a 345 μm acrylate coating. A dark nylon jacket then encloses the cable and protects the fibre from ambient light, humidity and mechanical breakage. The longitudinal dimensions are different in the case of the two facilities to meet their specific requirements.

At the ASLS, two 125 m cables cover the full storage ring with some margin to extract the generated light out of the accelerator tunnel, to where the electronics is located. In the following sections we will refer to the ASLS fibres as the RF fibre and scraper fibre according to the device they are protecting. The two light extraction points were located in sectors 2 and 9. The fibres were located in the horizontal plane on the inner side of the rectangular beam vacuum chamber, approximately 5.5 cm from the beam. At the TBL, a 28 m long signal fibre is located on top of the beam vacuum chamber, some 28 cm from the beam. The light is directed out of the tunnel via a 25 m and 75 m extraction fibres at the downstream and upstream ends respectively. Two identical

optical fibres are installed parallel to these extraction fibres to subtract any potential background light not generated in the TBL itself. A sketch of the fibre installation is also illustrated in Figure 1.

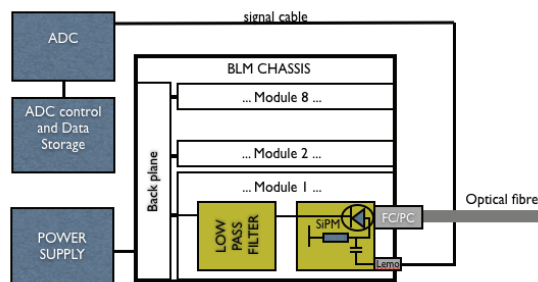


Figure 2: Schematic view of the oBLM read out.

The front-end electronics, shown schematically in Figure 2, features custom made Silicon Photomultiplier (SiPM) readout cards connected to a backplane that distributes the bias voltage for the sensors, the voltage for amplification and provides the grounding. A detailed description of the individual modules, that include low pass filters in the bias voltage input and an AC coupled signal readout can be found in [7]. The SiPMs are Hamamatsu s12572-015C detectors selected for their fast response and wide dynamic range. The back-end electronics consists of analog to digital converters (ADC). In the case of the TBL system, the signals were read out via 8 channel SIS3320 cards with 250 MHz bandwidth, up to 1.25 GS/s sampling rate and 10 bit resolution controlled via VME crate. Two different digitizers, Acqiris cards U1071a and DC282, were used at ASLS. The specifications in terms of sampling rate, bandwidth and resolution were 1 GHz, 2GS/s and 8 bit for the former and 2 GHz, 2GS/s

and 10 bit for the latter. Both digitizers were connected to PCs that provided the processing power and data storage.

SINGLE BUNCH MEASUREMENTS

Two sets of single bunch measurements were performed at the ASLS storage ring as a reference for the studies presented in this contribution.

Understanding of Beam Losses

One single bunch was injected into an empty machine and the beam losses during the first turn were investigated. Figure 3 presents a multi-peak structure due to losses occurring at various locations in the scraper (top) and RF (bottom) fibres respectively. Note that due to the better position resolution achievable with photons traveling upstream the fibre [8], only this output is studied throughout this contribution.

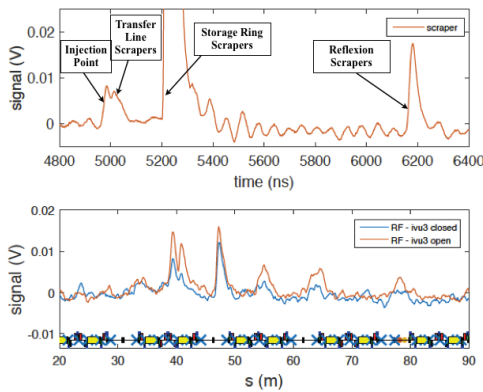


Figure 3: First turn losses observed in the scraper (top) and RF (bottom) fibres.

A sketch of development of signals in the scraper fibre during the first turn is shown in Figure 4. Electrons are kicked horizontally from the transfer lines into the storage ring, generating losses around the injection point (x_1). This produces a photon pulse in the scraper fibre that travels towards the upstream end with velocity $v_Q = c/n_Q$, with $n_Q = 1.47$ representing the (average) refractive index of quartz in the wavelength range of interest (200-900 nm) and c is the speed of light. The first detected light pulse in the scraper fibre shows a double peak behaviour, with the second peak attributed to showers generated in the beam scrapers of the transfer lines. Thereafter, the beam travels for a sector and exits the fraction of the storage ring covered by the scraper fibre. Once the beam reaches sector 9 it runs again parallel to the scraper fibre and in sector 11, it hits the beam scraper generating more showers (at position x_2). This process is illustrated in Figure 4. The arrival time of photons generated at x_1 and x_2 at the SiPM can be calculated as:

$$t_1 = t_0 + x_2/v_Q \tag{1}$$

and

$$t_2 = t_0 + L/c + x_1/v_Q \tag{2}$$

where t_0 represents the time at injection and L is the distance between the two loss points measured in the direction of the beam. Subtracting the two equations above and using the relation $\Delta x = x_1 - x_2 = L_{RING} - L$, with $L_{RING} = 216$ m, we can calculate the distance between the two points as:

$$\Delta x = \frac{L_{RING} - c\Delta t}{1 + n_Q} \tag{3}$$

For a measured temporal distance between the peaks x_1 and x_2 of $\Delta t = 220$ ns a distance of $\Delta x = 60.7$ m is calculated, which corresponds to the distance between the injection point and the beam scrapers. A third peak at $t \sim 6.2 \mu s$ is also observed. This is attributed to the large number of photons generated at the beam scrapers that travel to the downstream end of the fibre and partly reflected to the upstream end.

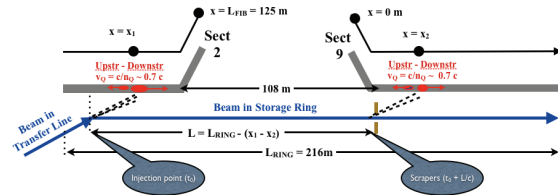


Figure 4: Sketch of the development of signals in the scraper fibre during the first turn.

In the case of the RF fibre the interpretation of the signals is much simpler as the beam travels, without interruption, parallel to the fibre. Thus, the distance between two loss points can be calculates as:

$$\Delta x = \frac{c\Delta t}{1 + n_Q} \tag{4}$$

Figure 3 shows, for the RF fibre, a multi-peak structure that is attributed to a modulation of the transverse beam size. A mockup of the double bend achromat lattice overlaid on Figure 3 shows that the peaks correspond to the quadrupole position. The effect of an opened and closed IVU3 located at approximately 30 m after the injection point, is also shown in the graphic. When closed during the first turn it limits losses downstream, while when open more downstream losses are observed. Note that in the bottom figure, the x axis has been scaled to position via Eq. (4).

Intrinsic Time Resolution

In order to understand the intrinsic time resolution of the system the raising edge of the signals generated at the beam scrapers, as a well defined loss location, were studied. An individual bunch was injected with the RF bucket in which it was injected incremented on every injection. The leading edge of 1000 pulses is presented in Figure 5 with a different color for each bucket. Note that, the oBLM system is clearly capable of disentangling signals separated by 2 ns on a shot by shot basis.

To probe the response of the system to signals separated by shorter time periods the RF phase of the Booster was shifted by 180° with respect to that of the storage ring. The arrival

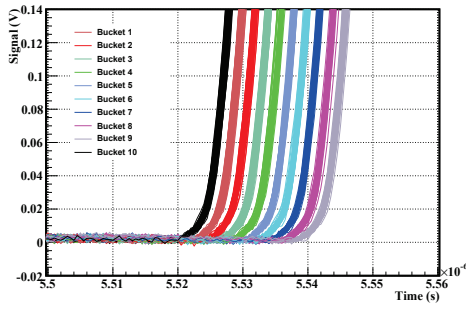


Figure 5: Leading edge of signals generated at the scrapers by single bunches injected into buckets 1 to 10.

time of the photons to the upstream end of the fibre was calculated as the temporal value for which the oBLM signal reached $V_{thr} = 100$ mV. To accomplish that, the sample value closer to V_{thr} was taken as a central value for an exponential fit ($V = a \cdot e^{b \cdot t}$) that included two samples (acquired at a 2 GS/s rate) on each side.

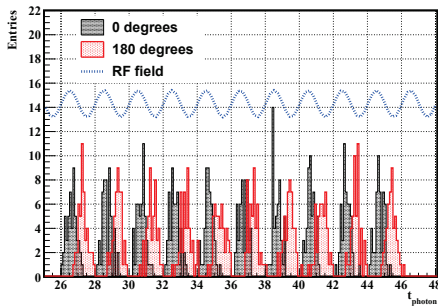


Figure 6: Photon arrival time at the upstream end of the fibre.

Figure 6 shows the distribution of photon arrival time for 0 (black) and 180° (red) phase shift as well as the modulation of the 500 MHz RF field. A slight overlap of the distributions tails for both RF phase shifts is observed. The distance between the mean values of the single bucket distribution is lower than the expected 1 nanosecond. This effect is not understood and is still under investigation. The overall time resolution of the system is calculated based on the quantity $\Delta t = t_{photon} - t_{mean}$, where t_{photon} is the arrival time as described above and $t_{mean} = t_{off} + n \cdot T_{RF}$ is the central value of the n^{th} bucket. For the Δt distributions shown in Figure 7, t_{off} is chosen as the mean value of the gaussian corresponding to the fifth bucket. It can be seen that the one sigma resolution obtained for both phases are compatible with each other and less than 300 ps.

MULTI BUNCH MEASUREMENTS

Multi bunch measurements conducted at both ASLS and CTF3 were performed to understand the behaviour of the oBLM system with longer pulses.

Multi Bunch Losses at ASLS

First turn losses were again investigated at the storage ring of the synchrotron but this time the length of the in-

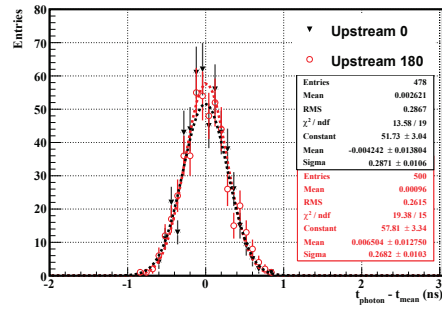


Figure 7: Δt distribution and gaussian fit for 0 and 180 degree phase shift between booster and storage ring RF.

jected pulse was modified. Signals in the oBLM system were studied with trains of 15, 25, 50 and 75 bunches which corresponds to 30, 50, 100 and 150 ns pulse length. As expected, for losses sufficiently separated in position, loss structure is still observable (Figure 8). In the scraper fibre the two peaks corresponding to the injection point and the beam scrapers are still observable with the time difference between the raising edge of the observed peaks matching the distance calculated in the single bunch case.

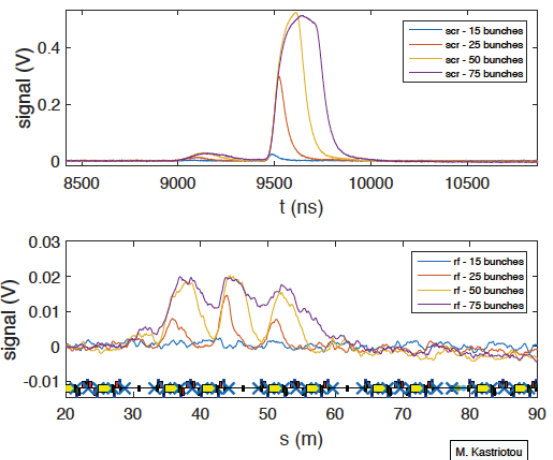


Figure 8: Multi bunch generated signals in the upstream scraper (RF) fibre at the top (bottom).

However, determining the location of beam losses signals close in time is more challenging. This is illustrated in the RF plot of Figure 8, where losses are produced at quadrupoles separated in some cases by less than 2 metres. Without any further processing, the peak structure of the oBLM signals is more and more spread out as the pulse length is increased. This limitation may be overcome deconvoluting the signals by taking into account the non flat intensity profile in a bunch train. Measuring the bunch by bunch charge in a full train with the wall current monitor located after the gun, it is observed that the first few bunches carry very low charge. The intensity increases along the train and it becomes constant after the 15th bunch has been injected.

Long Electron Pulses

A final test with a 1 μ s long beam pulse was conducted at the TBL in CTF3. The bunch spacing was defined by the 3GHz RF frequency and the measured peak current was 3 A. Beam losses during standard operation, i.e. with nominal quadrupoles settings, were measured and compared to those generated when turning off various magnets. The signals induced by shower generated at the TBL were computed by subtracting the signals observed in the background fibre to those measured in the TBL fibre. This is illustrated in Figure 9 for the case of nominal beam transmission, where it is shown that both the signal and background fibres carry an almost identical amount of light in the first (~ 150) nanoseconds. The very low signal level is attributed to observing only a very small fraction of beam loss and to attenuation in the 75 meter long extraction fibre at the upstream end.

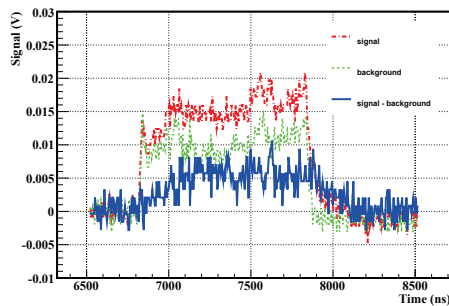


Figure 9: BLM signals observed during nominal beam transmission at the TBL.

During this experiment, the location of beam losses was determined by looking at the oBLM signals and comparing it to the intensity signal of the BPMs (1-16) along the TBL, as shown in Figure 10. At the top of the graph, the x axis indicates relative position in the line as demonstrated by the 1.4 meter distance between consecutive points. In the nominal case, there are no beam losses observed to within the accuracy of the devices. This is consistent with the low signals observed in the oBLMs (5 mV peak) for these quadrupole settings. When successively switching off specific quadrupoles, the first measured beam loss is observed with the BPM located immediately downstream of the next quadrupole.

The top of Figure 10 shows the leading edge of the (background subtracted) oBLM signal. Each trace is the average of 100 shots acquired for each quadrupole setting, with background subtraction performed on a shot-by-shot basis. At the top of the graph, the axis represents the relative position along the line as calculated by Eq. (4). It can be seen that there is very good agreement between the loss location calculated from the oBLM rising edge and that given by the BPM signals, with localisation down to below 2m easily achieved.

CONCLUSION

An oBLM system with SiPM based optical readout has been installed in the storage ring of the Australian Syn-

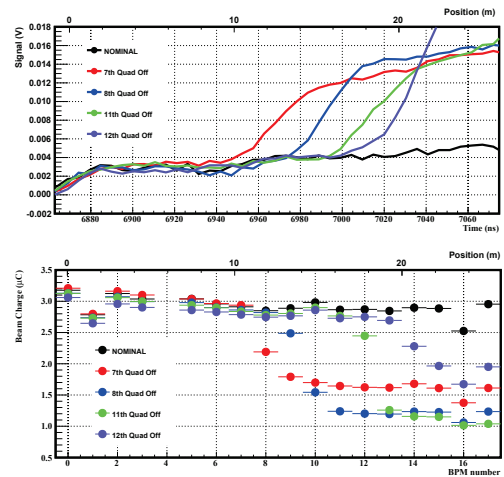


Figure 10: Leading edge of the BLM signals (top) and current measured by the BPMs (bottom) at the TBL.

chrotron and at the TBL of CTF3 at CERN. The former system has been used to perform single bunch studies that have shown the system to have an intrinsic time resolution for the system better than three hundred picoseconds and set the ground for multi bunch studies. The latter has been used to experimentally demonstrate, for the first time to the best of our knowledge, that reconstructing the original location of a beam loss is also possible with longer electron pulses.

ACKNOWLEDGMENT

The authors of this paper would like to thank the operators of CTF3 and the ASLS for their invaluable help on the execution of the experiments necessary for obtaining these results. This work has been partly funded by the Royal Society via the Intentional Exchange Scheme project PPR10353.

REFERENCES

- [1] T. Obina, "Optical fibre based Beam Loss Monitoring for electron storage rings", IBIC13, Oxford, September 2013.
- [2] J. Boldeman et al., "The physics design of the Australian synchrotron storage ring", Nucl. Instr. and Meth., A 521, 2004.
- [3] CLIC Collaboration, "A multi-TeV linear collider based on CLIC technology", CLIC Conceptual Design Report. Volume 1 Technical Report. CERN, Geneva 2012.
- [4] E. Nebot et al., "Measurement of beam losses at the Australian synchrotron", IBIC14, Monterrey, September 2014.
- [5] R. Lillestrol et al., "Experimental results from the Test Beam Line in the CLIC Test Facility 3", IPAC13, Shanghai, 2013.
- [6] J. J. Garcia-Garrigos et al., "Design and Construction of an inductive pick-up for beam position monitoring in the test beam line of CTF3", EPAC2008.
- [7] E. Nebot et al., "Studies of SiPM nonlinearities and transients at short light pulse detection", LA3NET, Mallorca, March 2015.
- [8] J. van Hoorne, "Cherenkov fibers for Beam Loss Monitoring at the CLIC Two Beam Module", CERN-THESIS-2012-112.